

# Two cases of phase-shifting interferometry for wave front recovery from heterodyne hologram storage: piezoelectric transducer and modulation of polarization

G. RODRÍGUEZ-ZURITA<sup>1\*</sup>, J.F. VÁZQUEZ-CASTILLO<sup>1</sup>, N.I. TOTO-ARELLANO<sup>2\*</sup>,  
G. CALDERÓN-HERNÁNDEZ<sup>1</sup>, E. BAROJAS-GUTIÉRREZ<sup>1</sup>

<sup>1</sup>Benemérita Universidad Autónoma de Puebla, Pue. 72570, México

<sup>2</sup>Universidad Tecnológica de Tulancingo, Hgo. 43642, México

\*Corresponding author: gzurita@cfm.buap.mx; ivantotoarellano@hotmail.com

Heterodyne holographic interferometry is a well-known interferometric technique for high precision measurements of the phase difference between two recorded wave fronts. These wave fronts are typically registered at a given distance from the object under inspection. Although the affinity of heterodyne techniques with the phase-shifting ones is immediate, reports on concrete implemented set-ups from the former type of techniques as adaptations into the second type seems to be not so widely spread as convenient. To illustrate this point, in this communication we demonstrate two phase-shifting methods as applied to heterodyne holograms, each variant using a different shifting method for phase shifting. One method is based on a conventional piezoelectric stack transducer and the other method comprises modulation of polarization. The alternatives that these two techniques offer could be of direct benefit in dynamic holography.

Keywords: holographic interferometry, phase-shifting, polarization.

## 1. Introduction

Heterodyne holographic interferometry (HHI) was described by DÄNDLIKER [1, 2] and it is a well-known optical holographic interferometry technique claiming precision phase measurements of the order of  $\lambda/1000$  [1], where  $\lambda$  is the wavelength of the illuminating light source employed. Basically, two states of a given object are to be compared by recording two respective holograms, each one with a different reference wave. A digital approach to HHI has been described and experimentally demonstrated by solving the related problems emerging when substituting high-resolution photographic emulsions with a 2-dimensional array of photodetectors [3]. In this approach, before a proper numerical reconstruction by demodulation of irradiances, a number of digital holograms

(at least three for one wave front) must be recorded in sequence. More recent applications using digital HHI have been reported [4]. But optical HHI techniques have, on the other side, a close relation with phase-shifting interferometry (PSI, which comprises techniques belonging to the once called quasi-heterodyne interferometry). In the following, high resolution photographic storage is considered to emphasize some advantages accompanying such a relation. Firstly, only two wave fronts are to be recorded. Read-out is with PSI techniques to be done. Under such conditions, it is in this communication that we demonstrate two PSI methods as applied to optical heterodyne holograms, each one of the two proposals using a different shifting method for phase shifting. The first of them employs a conventional piezoelectric stack transducer (PZT) [2] while the second one uses modulation of polarization (MP) [5]. As a second advantage, by MP in particular, an amplitude-multiplexing procedure can be implemented to obtain three or even more interferograms using only the original recording. For the purposes of this paper, an isotropic recording medium is assumed. The two advantages above referred can be of benefit to the experimental analysis of fast processes, because some conclusions of this work could be useful in dynamic holography after adapting proper polarization techniques of recording.

## 2. Experimental set-up

According to DÄNDLIKER [1], upon proper reconstruction of the recording of two wave fronts in two exposures, each one performed with a different reference wave (Fig. 1), an interference pattern can arise which results (as opposite to a single-reference double-exposure hologram) in a pattern which is able to be spatially modulated [1, 2]. This is essentially due to the independence of the reference waves (and thus, the reconstruction waves), which makes possible to introduce relative phase-shifts using a transducer in only one beam at least. Such shifts can be achieved with a PZT placed in the path of one reconstructing beam. Also, in order to achieve the same type of a shift, it is possible to modulate both reference beams differently with some additional advantages. This can be done with MP by imposing circular polarization of opposite sign for each reconstruction beam and detecting the resulting interference pattern with a linear polarizer whose transmission axis is adjusted at the appropriate angle according to the desired shift [5].

## 3. Recording of heterodyne holograms

Some heterodyne holograms were recorded on photographic emulsions closely following Dändliker prescription [1], as shown in Fig. 1. This includes the use of two different references  $R_1$  and  $R_2$  for each one of two different exposures (opening and closing the main switch) at respective times  $t_1$  (switch 1 open, switch 2 closed) and  $t_2$  (switch 1 closed, switch 2 open). Care was taken for the radius of curvature of both references

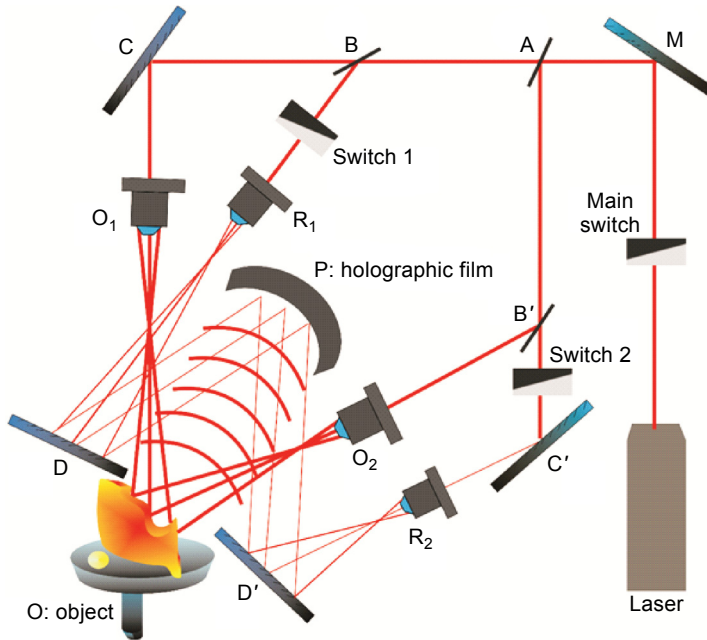


Fig. 1. Set-up used for recording a heterodyne hologram. A, B, B' – beam splitters; M, C, C', D, D' – plane mirrors, and  $O_1$ ,  $O_2$ ,  $R_1$ ,  $R_2$  – microscope objectives. He-Ne-laser at 632.8 nm.

to be the same as possible. Not exactly symmetrical angles of the reference waves with respect to the normal of the recording media were chosen, so as to avoid overlapping between different reconstructions. At the same time, however, the angle between references should not be very large, so as to get interference fringes during reconstruction of spatial frequencies with values low enough to be resolvable during detection for PSI. Thus, the angle between references was chosen slightly larger than the angular size of the object [1]. Two additional beams were used to illuminate a reflective object O from opposite sides during both exposures, thus avoiding undesirable sharp shadowing ( $O_1$  and  $O_2$  beams). A He-Ne laser was used as the illuminating source (10 mW at 632.8 nm). Optical paths for each of the four beams were adjusted to be equal. The object O was placed on a small table during both exposures. However, to introduce rather arbitrary but small translations and rotations in the object, a small steel ball was placed on the table only during one of the exposures (circle on the stage close to the object, Fig. 1).

For read-out, two reconstruction waves similar to the reference waves were used at the same angles used for references. Fine adjustment of the resulting images can be done until fringes appear on the field of view. Figure 2 shows an example of a test object and the reconstructed waves with their obtained interference fringes. In this case, the object consists of a fish replica carved from a piece of a local variety of onyx (known

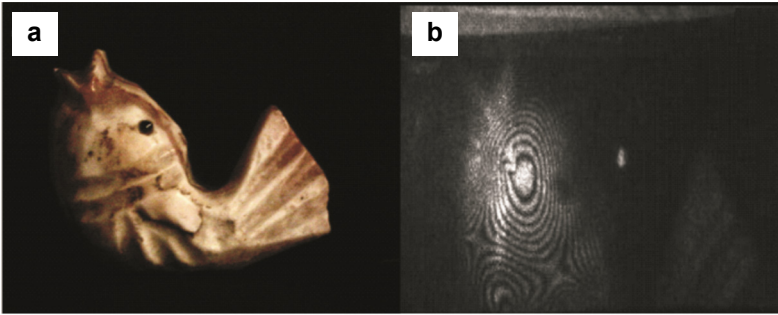


Fig. 2. Original main object (a). Interference pattern located close to the reconstructed object (the object is shown slightly out of focus for better detection of interference fringes) as seen with a CCD camera at 632.8 nm (b). It becomes possible to spatially modulate the pattern by proper modulation of (at least) one of the reconstructing beams.

as *tecali*), Fig. 2a. An interference pattern appears located at some distance from the object (Fig. 2b). The fringes of the pattern are able to be shifted by modulating whichever one of the reference waves.

#### 4. Experimental results with phase-shifting

The following subsections discuss the two set-ups for reconstruction and the respective procedures for phase extraction. Section 4.1 refers only to the PZT modulation set-up, while Section 4.2 describes the algorithm used for phase extraction. This last description is common for both procedures. Section 4.3 describes the basics of MP modulation and Section 4.4 describes the corresponding set-up implementation.

##### 4.1. Phase-shifting and extraction with PZT

Figure 3 shows the reconstruction of the two scalar wave fronts  $W_1$  and  $W_2$  recorded at times  $t_1$  and  $t_2$ , where

$$W_l = W_{0l} \exp \left\{ -i \left[ \mathbf{k}_l \cdot \mathbf{r} - \omega t + \varphi_l(\mathbf{r}) \right] \right\}, \quad l = 1, 2 \quad (1)$$

with  $\mathbf{k}_l$  denoting the  $l$ -wave vector having  $|\mathbf{k}_l| = k$  as the wave number,  $\omega_1 = \omega_2 = \omega$  denoting the wave frequency and  $\varphi_l(\mathbf{r})$  denoting the respective phase departures from plane waves during each exposure. Also,  $\mathbf{r} = (x, y, z)$ . Thus, dropping the dependence on  $z$ , assuming a recording over a fixed plane and including linear contributions of  $x$  and  $y$  in  $\varphi$  due to possible not perfect collinearity of the wave vectors (tilts), an interference pattern after simultaneous reconstruction appears as given by

$$I_i = \|W_1 + W_2\|^2 = B + A \cos \left[ \xi_i - \varphi(x, y) \right] \quad (2)$$

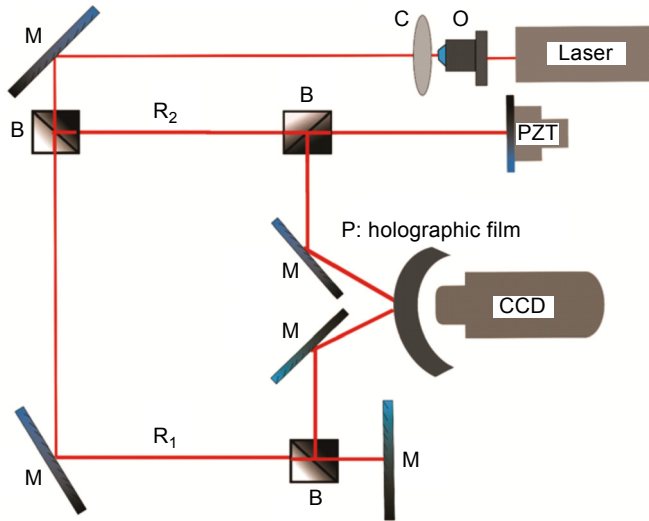


Fig. 3. Experimental set-up for a read-out of a heterodyne hologram introducing phase-shifts in arm  $R_2$  for phase-extraction. M – plane mirrors, C – collimator, O – microscope objective, B – beam splitter, PZT – piezoelectric stack, CCD – digitizing camera. Angles of the reconstruction waves were not really symmetrical with respect to the normal of the recording media.

where  $\zeta_i$  is a known, purposely introduced phase-shift of a set of  $M$  interferograms, with  $i = 0, \dots, M - 1$ . In our case  $M = 4$ . Also,  $B = W_{01}^2 + W_{02}^2$ ,  $A = 2W_{01}W_{02}$  and  $\varphi(x, y) = \varphi_1(x, y) - \varphi_2(x, y)$  is the phase difference of interest.

Figure 2b shows an example of such an interferogram generated with simultaneous reconstruction;  $\zeta_m$  is first introduced with a plane mirror attached to a calibrated piezoelectric stack driven by a computer (PZT in Fig. 3). Each  $I_i$  is captured by a CCD digitizing camera. As usual in PSI, the interferograms serve to construct a system of linear equations to obtain  $\tan[\varphi(x, y)]$ . A four pattern algorithm was applied to extract the wrapped phase and the resulting unwrapped phase  $\varphi(x, y)$  is shown in Fig. 4 for five different views (azimuth angle  $\alpha$ ).

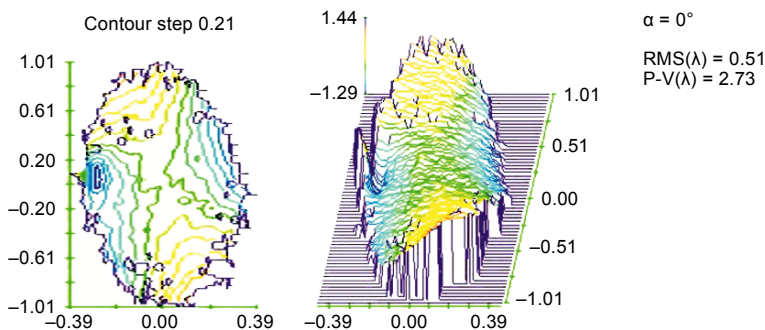


Fig. 4. To be continued on the next page.

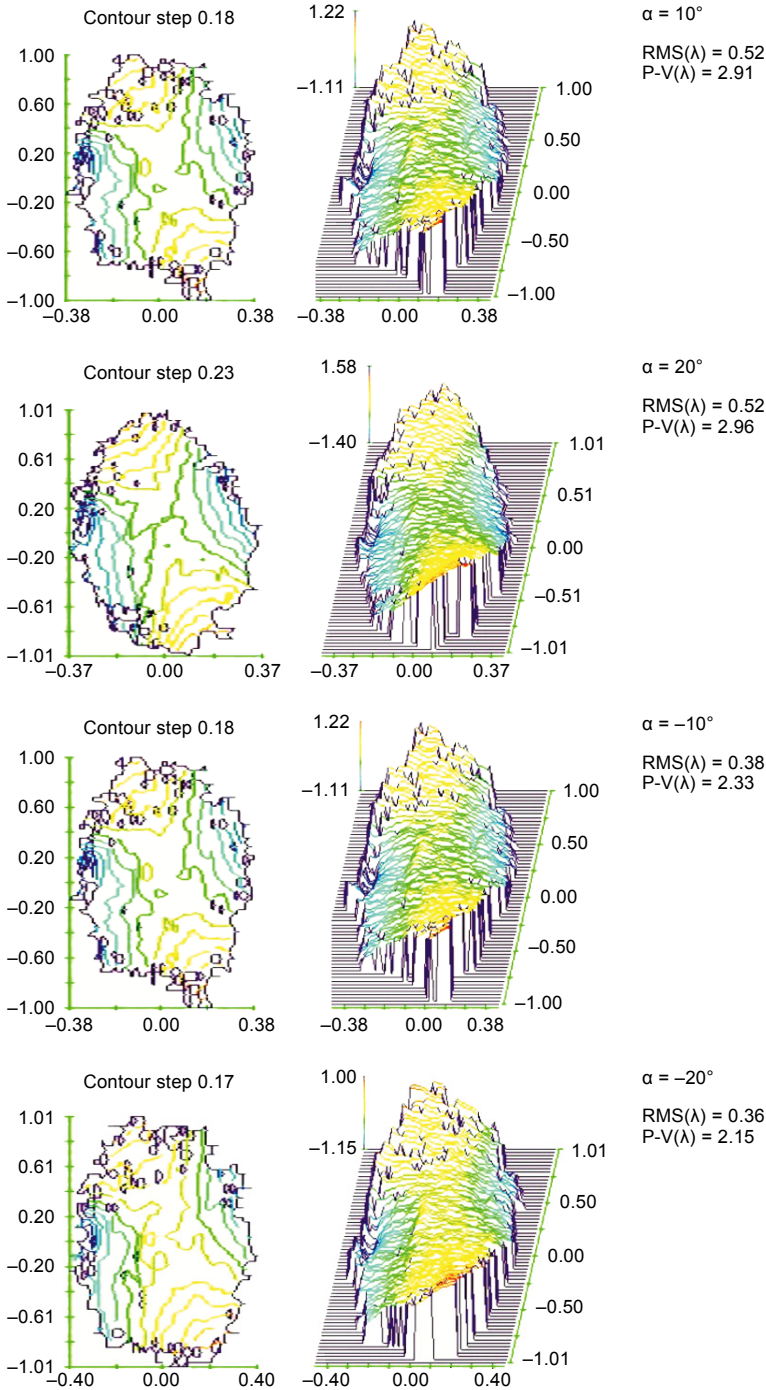


Fig. 4. Typical wave front extractions (contour and surface plot) using a 4-interferogram procedure at several different view (azimuth angles  $\alpha$ ). P-V denotes peak-to-valley values in wavelengths (632.8 nm).

## 4.2. Phase processing algorithm

Generation of known phase shifts of  $0$ ,  $\pi/2$ ,  $\pi$  and  $3\pi/2$  can be done by calibrating the PZT properly. The obtained four interferograms can be represented as:

$$I_1(x, y) = B + A \cos[\varphi(x, y)] \quad (3a)$$

$$I_2(x, y) = B + A \sin[\varphi(x, y)] \quad (3b)$$

$$I_3(x, y) = B - A \cos[\varphi(x, y)] \quad (3c)$$

$$I_4(x, y) = B - A \sin[\varphi(x, y)] \quad (3d)$$

Phase reconstruction is performed using the four step phase shifting algorithm, so the wrapped phase can be obtained from the following equation:

$$\varphi(x, y) = \tan^{-1} \left[ \frac{I_2(x, y) - I_4(x, y)}{I_1(x, y) - I_3(x, y)} \right] \quad (4)$$

After removing the  $2\pi$  ambiguity by means of a phase unwrapping process, the optical phase can be obtained; the method used for unwrapping this phase data was a quality-guided path following method [6–9].

## 4.3. Phase-shifting with MP

In general, the polarization states of two optical classical disturbances can be determined by

$$\mathbf{J}_L = \frac{1}{\sqrt{2}} \begin{bmatrix} 1 \\ \exp(i\alpha') \end{bmatrix} \quad (5a)$$

$$\mathbf{J}_R = \frac{1}{\sqrt{2}} \begin{bmatrix} 1 \\ \exp(-i\alpha') \end{bmatrix} \exp[i\varphi(x, y)] \quad (5b)$$

where  $\alpha'$  is some phase introduced by a plate retarder. New disturbances emerge from a linear polarizer whose transmission axis forms the angle  $\psi$  with transmission given by

$$J_\psi^l = \begin{bmatrix} \cos^2(\psi) & \sin(\psi) \cos(\psi) \\ \sin(\psi) \cos(\psi) & \sin^2(\psi) \end{bmatrix} \quad (6)$$

changing the output polarization states to  $\mathbf{J}' = J_\psi^l \mathbf{J}_L$  and  $\mathbf{J}'' = J_\psi^l \mathbf{J}_R$ .

Then, irradiance from the superposition of both states can be written as

$$\begin{aligned} \|\mathbf{J}_T\|^2 &= \|\mathbf{J}' + \mathbf{J}''\|^2 \\ &= 1 + \sin(\psi) \cos(\alpha') + A(\psi, \alpha') \cos\left[\zeta(\psi, \alpha') - \varphi(x, y)\right] \end{aligned} \quad (7)$$

The phase shift  $\zeta(\psi, \alpha')$  so generated is given by

$$\zeta(\psi, \alpha') = \operatorname{atan}\left[\frac{\sin(2\psi) \sin(\alpha') + \sin^2(\psi) \sin(2\alpha')}{\cos^2(\psi) + \sin^2(\psi) \cos(2\alpha') + \sin(2\psi) \cos(\alpha')}\right] \quad (8)$$

with  $A(\psi, \alpha')$  which can be written as

$$A(\psi, \alpha') = 1 + \sin(2\psi) \cos(\alpha') \quad (9)$$

These relations contain a special case of two circular polarizations with opposite signs because, with  $\alpha' = \pi/2$ ,

$$\zeta(\psi, \pi/2) = 2\psi \quad (10a)$$

$$A\left(\psi, \frac{\pi}{2}\right) = 1 \quad (10b)$$

Thus, the introduction of a phase shift can be done with circular polarizations and detection with a linear polarizer at the angle  $\psi$  given by Eq. (8) for the general case (or Eqs. (10) for the particular case of circular polarization). Such phase-shifting technique has been earlier used for the design of micropolarizers and  $\alpha' = \pi/2$  in single-shot phase shifting holography [10]. Although the shifts we just described can be sequentially introduced, it is possible to perform several shifts at the same time by using appropriate multiplexing of interference fields [5]. Using phase-grating multiplexing, for example, the number of interferograms is not limited to 3 or 4, and no specialized microarray fabrication is required, as already demonstrated [11]. The system neither requires a very good coincidence between similar pixels of different interferograms. In our case, because the subject is not moving and the wave fronts are stored, testing measurements can be done in sequence for simplicity.

#### 4.4. MP for phase-extraction

Figure 5 shows the wave front reconstruction set-up for the case of MP. MP is achieved by imposing circular polarization of the opposite sign in each reconstruction beam. The phase shift was sequentially performed adjusting a linear polarizer at an angle  $\psi_i$ , with  $i = 0, 1, 2, 3$  as before. The phase shift  $\zeta_i(\psi_i, \alpha')$  is given by Eq. (8) (or Eqs. (10)). Phase-shifting produces corresponding fringe shifts by only adjusting the transmission angle  $\psi_i$  of the linear polarizer. Once the transmission axis angle  $\psi_i$  of the polarizing filter is determined, no further adjustment is needed. Each interferogram is captured



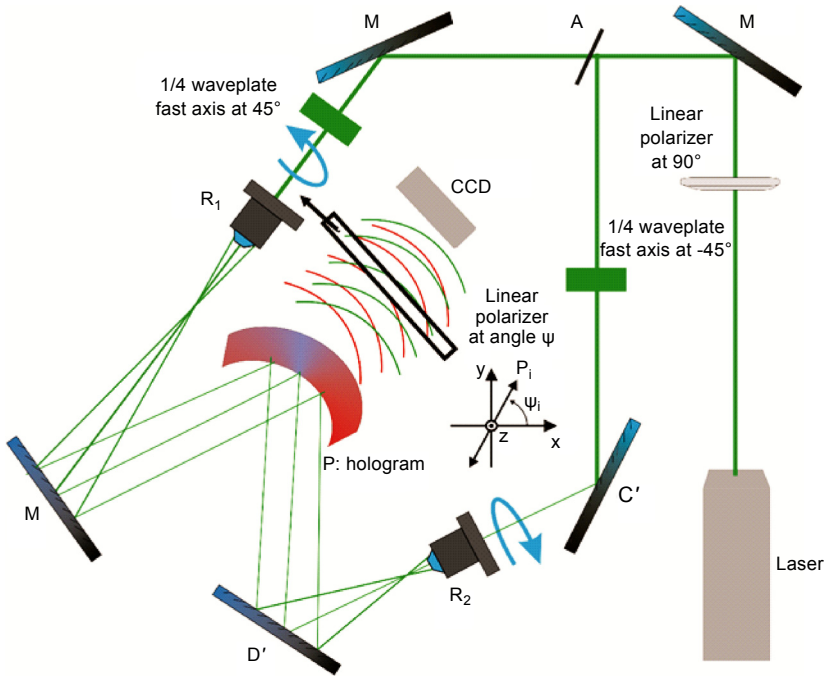


Fig. 5. Experimental set-up for phase extraction by employing MP. Circular polarizations with opposite directions of rotation were imposed in each reconstruction wave by means of proper waveplates. CCD – digitizing camera; M, C', D' – plane mirrors; R<sub>1</sub>, R<sub>2</sub> – microscope objective; A – beam splitter; P – polarizer.

with a CCD camera and stored. Interferograms need to be normalized to their maximum value prior to be used in the described algorithm calculating the wrapped phase. Figure 6 shows two sets of four interferograms, each taken at a different viewing angle.

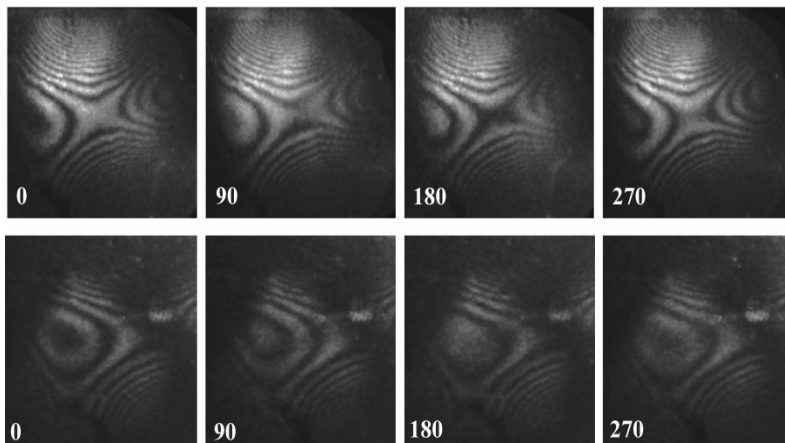


Fig. 6. Two sets of four interferograms taken at a two different viewing angles ( $\lambda = 532 \text{ nm}$ ).

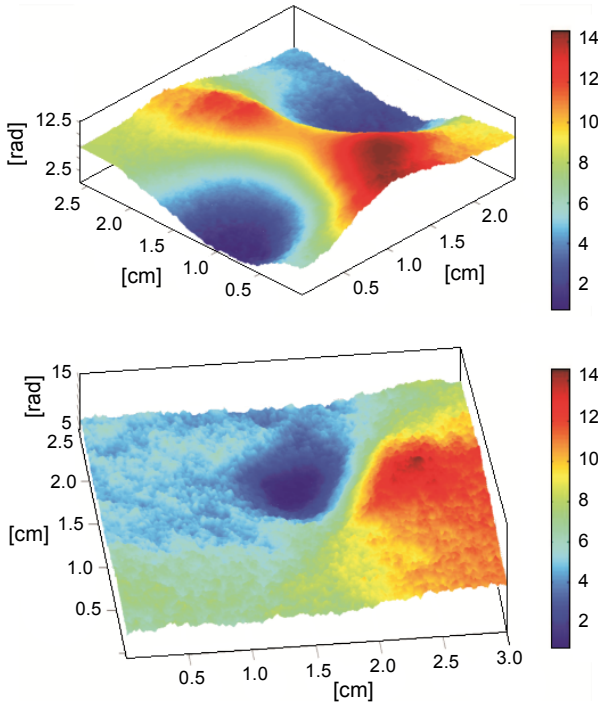


Fig. 7. Typical wave front extraction (phase) using a 4-interferogram procedure at two different view angles ( $P\text{-}V(\lambda) \approx 2.387$ ,  $\lambda = 532$  nm).

The unwrapped wave front difference between the registered wave fronts is plotted in Fig. 7. A preliminary report on this technique was presented elsewhere [12]. Extraction of the phase encoded in optically stored heterodyne holograms is thus possible with the two tested variants of PSI [13, 14]. The heterodyne hologram practically behaves as a beam splitter with memory, ready to be a part of a phase-shifting interferometer. Due to the employment of different algorithms, units and wavelengths, only a qualitative comparison is directly possible at this stage. However, surface plots and ranges seem to be similar for both techniques. Collected data were also consistent and reproducible (Figs. 4 and 7).

This also means that the recording methods proper of HHI plus MP can be considered as an eventual choice for phase extraction other than Fourier transform interferometry [15], for example, especially when rather small phase-variations (within a fringe, for example) are to be measured or when no carrier-frequency becomes easily available. Moreover, it is worthy to recall that interferometric parameters  $B$  and  $A$  can also be determined under the same system of linear equations that gives  $\varphi(x, y)$ . For objects with arbitrary shapes and absorptions, amplitudes  $W_{0l}$  do change spatially in accord with the object's geometry. These changes affect the values of  $A$  and  $B$ . Thus, the eventual knowledge of  $B$  and  $A$  would make it easier to establish links between the resulting

phase differences and the geometry of the object if desired. This feature would be similar for both modulation techniques.

## 5. Final remarks

Migration in the read-out from the heterodyne regime to the phase-shifting regime can be easily done under several variants of shifting techniques. Considering shifting calibration, PZT has to be calibrated for each interferometer adjustment, which means a new calibration for each fringe adjustment whereas MP, once calibrated for one interferogram, is already calibrated for another one appearing under a different adjustment. Moreover, MP is able to render several phase-shifted interferograms in one-shot by using grating interferometry multiplexing methods.

Additionally, when using a film as the recording medium, it tends to act as a membrane, so it is very sensitive to acoustical vibrations. These sensitivity can be shared by other recording media as well. The MP technique has the advantage of not using mechanical elements in the interferometric system that could generate vibrations while performing the phase shifts. This allows to perform the calculation of the optical phase without the common errors that could be generated by vibrations in the holographic system [5, 10, 11].

*Acknowledgements* – This research was partially supported by The Initiative for the Creation of the First Optics and Photonics Engineering undergraduate program in México. One of the authors (EBG) acknowledges CONACYT for support. The author would like to thank the anonymous reviewers for their valuable comments and suggestions to improve the quality of the paper.

## References

- [1] DÄNDLIKER R., *Heterodyne holographic interferometry*, [In] *Progress in Optics*, [Ed.] E. Wolf, Vol. 17, North-Holland Publishing, Amsterdam, 1980, pp. 1–84.
- [2] KREIS T., *Handbook of Holographic Interferometry: Optical and Digital Methods*, Wiley-VCH Verlag, Weinheim, 2005.
- [3] LE CLERC F., COLLOT L., GROSS M., *Numerical heterodyne holography with two-dimensional photo-detector arrays*, *Optics Letters* **25**(10), 2000, pp. 716–718.
- [4] SUCK S.Y., COLLIN S., BARDOU N., DE WILDE Y., TESSIER G., *Imaging the three-dimensional scattering pattern of plasmonic nanodisk chains by digital heterodyne holography*, *Optics Letters* **36**(6), 2011, pp. 849–851.
- [5] RODRIGUEZ-ZURITA G., MENESES-FABIAN C., TOTO-ARELLANO N.I., VÁZQUEZ-CASTILLO J.F., ROBLEDO-SÁNCHEZ C., *One-shot phase-shifting phase-grating interferometry with modulation of polarization: case of four interferograms*, *Optics Express* **16**(11), 2008, pp. 7806–7817.
- [6] GHIGLIA D.C., PRITT M.D., *Two-Dimensional Phase Unwrapping: Theory, Algorithms, and Software*, Chapter 4, Wiley, New York, 1998.
- [7] SERVIN M., ESTRADA J.C., QUIROGA J.A., *The general theory of phase shifting algorithms*, *Optics Express* **17**(24), 2009, pp. 21867–21881.
- [8] KERR D., KAUFMANN G.H., GALIZZI G.E., *Unwrapping of interferometric phase-fringe maps by the discrete cosine transform*, *Applied Optics* **35**(5), 1996, pp. 810–816.

- [9] GHIGLIA D.C., ROMERO L.A., *Robust two-dimensional weighted and unweighted phase unwrapping that uses fast transforms and iterative methods*, Journal of the Optical Society of America A **11**(1), 1994, pp. 107–117.
- [10] NOVAK M., MILLERD J., BROCK N., NORTH-MORRIS M., HAYES J., WYANT J., *Analysis of a micro-polarizer array-based simultaneous phase-shifting interferometer*, Applied Optics **44**(32), 2005, pp. 6861–6868.
- [11] RODRIGUEZ-ZURITA G., TOTO-ARELLANO N.I., MENESES-FABIAN C., VÁZQUEZ-CASTILLO J.F., *One-shot phase-shifting interferometry: five, seven, and nine interferograms*, Optics Letters **33**(23), 2008, pp. 2788–2790.
- [12] RODRIGUEZ-ZURITA G., VÁZQUEZ-CASTILLO J.F., TOTO-ARELLANO I., MENESES-FABIAN C., JIMÉNEZ-MONTERO L.E., *Modulation of polarization in interferometric holography and two references*, Advanced Phase Measurement Methods in Optics and Imaging, Monte Verità, Locarno, Suiza, May 17–21, 2010, AIP Conference Proceedings, Vol. 1236, 2010, pp. 87–90.
- [13] TOTO-ARELLANO N.-I., SERRANO-GARCÍA D.-I., MARTÍNEZ-GARCÍA A., *Parallel two-step phase shifting interferometry using a double cyclic shear interferometer*, Optics Express **21**(26), 2013, pp. 31983–31989.
- [14] FLORES MUÑOZ V.H., TOTO ARELLANO N.-I., SERRANO GARCÍA D.I., MARTÍNEZ GARCÍA A., RODRÍGUEZ ZURITA G., GARCÍA LECHUGA L., *Measurement of mean thickness of transparent samples using simultaneous phase shifting interferometry with four interferograms*, Applied Optics **55**(15), 2016, pp. 4047–4051.
- [15] TAKEDA M., INA H., KOBAYASHI S., *Fourier-transform method of fringe-pattern analysis for computer-based topography and interferometry*, Journal of the Optical Society of America **72**(1), 1982, pp. 156–160.

*Received November 22, 2016  
in revised form February 24, 2017*